Int J Adv Manuf Technol (2016) 82:39–48
DOI 10.1007/s00170-015-7342-5

ORIGINAL ARTICLE

Friction stir lap welding of 5456 aluminum alloy with different sheet thickness: process optimization and microstructure evolution

Emad Salari[1] · **Mohammad Jahazi**[2] · **Alireza Khodabandeh**[1] · **Hadi Ghasemi Nanesa**[2]

Received: 15 December 2014 / Accepted: 19 May 2015 / Published online: 4 June 2015
© Springer-Verlag London 2015

Abstract The influences of friction stir welding process parameters on microstructure evolution and mechanical properties of lap-welded 5456 aluminum alloy plates with different thickness and temper conditions were investigated. The upper plate was 5 mm thick, cold rolled aluminum alloy 5456-T321 and the lower plate was 2.5-mm annealed sheet (5456-O). Four different pin geometry types (conical thread pin, cylindrical–conical thread pin, stepped conical thread pin, and flared-triflute pin tool) and two rotational speeds (600 and 800 rpm) were used to produce the joints. Microstructures and microhardness values in the weld nugget (WN), thermomechanically affected zone (TMAZ), and the heat-affected zone (HAZ) were examined and correlated with selected processing conditions. Specifically, the influence of tool geometry on the flow of the plasticized material in the nugget zone, extent of hooking defect, and mechanical properties (microhardness) of the FSW joints were documented and quantified. It was found that weld joints made by using the stepped conical thread pin tool produced a homogeneous microstructure with finer grain size (5.4 μm) and higher microhardness levels than the other tools. The optimum processing conditions resulting in sound and defect-free joints with highest mechanical properties were obtained with the stepped conical thread pin and 600-rpm rotational speed. The evolution of the microhardness in each region is characterized and related to processing conditions.

Keywords Friction stir welding · Aluminum alloy 5456 · Microstructure · Microhardness, weld nugget zone, and processing conditions

1 Introduction

Since its introduction in 1991 by The Welding Institute (TWI), friction stir welding (FSW) has been successfully applied to joining of aluminum alloys in the aerospace industry and is finding increasing applications to other materials and industries [1–3]. FSW is a solid-state joining method where a combination of in situ extrusion and forging processes are used to create metallurgical bonds without the need for reaching the melting point of any of the two adjoining materials. Frictional heat at the interface is generated through the rotation of a tool, composed of a pin and a shoulder, to generate enough frictional heat at the point of welding and induce the flow of material under the shoulder from one side to the other [4, 5].

One of the critical regions in an FSW joint is the one located at the center of the joint, commonly called weld nugget (WN). This region is the main lieu of mixing the materials from the opposite sides of the joint line and consists of very fine and equiaxed grains. The latter are formed as a result of multiple cycles of dynamic recrystallization due to the combination of high temperature and severe deformation applied in this region. Because of the tool rotation, the thermomechanical conditions are not similar in the advancing and retreating sides of the weld and, as a result, the

✉ Hadi Ghasemi Nanesa
hadi.ghasemi-nanesa.1@ens.etsmtl.ca

[1] Science and Research Branch, Islamic Azad University, 1477893855 Tehran, Iran

[2] Department of Mechanical Engineering, École de Technologie Supérieure, 1100 rue Notre-Dame Ouest, Montréal, QC H3C1K3, Canada

Table 1 Chemical compositions and microhardness measurement of the investigated alloys

Material	Chemical composition in wt%						Hardness at 200-g load (HV)
	Al	Mg	Mn	Cu	Fe	Si	
5456-H321	Bal	4.81	0.63	0.01	0.20	0.08	140
5456-O	Bal	4.79	0.50	0.02	0.18	0.12	89

microstructure of the material in the WN not identical on both sides of the weld, and therefore, different mechanical behaviors may be expected from each region in the WN. In addition to the WN, two other regions, heat-affected zone (HAZ) and thermomechanically affected zone (TMAZ), have also been identified as important locations in an FS weld that determine weld integrity [3, 6–10]. The combination of heat and deformation along the specific characteristics of each alloy (phase transformation, size and distribution of precipitates, etc.) can have a determining effect on the local mechanical properties and the global integrity of the weld joint.

In recent years, extensive studies have been carried out to quantify and document the effects of tool geometry on the mechanical properties of FSW on various kinds of aluminum alloys. For instance, in a study by A. Scialpi [11], the influence of shoulder geometry on microstructure and mechanical properties of FSW (hardness) of 6082 aluminum alloy was investigated. Results indicated that several factors including welding parameters, tool geometry, amount of surface contact between tool and material, and finally amount of heat input affected the mechanical properties of weld joints. Specifically, the authors found that hardness increased in the nugget zone, which was related to the formation of a very fine recrystallized microstructure. Other studies, carried out on a wide variety of precipitation-hardened aluminum alloys, the influence of FSW process parameters on the characteristics of the precipitates, and their impact on hardness profile have been investigated and mostly related to the local amount of heat generated by the rotating tool [11–15]. Therefore, tool geometry plays a critical role in obtaining defect-free FSW joints, and its selection has a direct impact in optimizing of the other process parameters such as tool rotation speed, tool advance, etc.

One of the main challenges in the optimization of the FSW process is the elimination of microscopic defects called kissing bonds. The latter are relatively continuous trails of the remnants of the oxide layers present at the joint interface which are not eliminated by the material stirring that takes place during the FSW process [6, 16, 17]. An extensive review of the literature indicates that tool geometry has a determining effect on the flow of the material beneath the shoulder and hence the elimination of the kissing bonds. However, due to the highly dynamic nature of the process and the difficulty in mathematically formulating and predicting material flow, the tool geometry optimization has been mostly based on experience [3, 5, 9, 11–15]. Specifically, Zhao et al. [2] found optimum joint properties in a 2014 aluminum alloy using a screw pitched taper stirrer pin. Chionopoulos et al. [5] reported that only conical pin gives defect-free welded joints in AA5083 aluminum alloy. Of special interest is also the work of Fujii et al. [12] on the effect of tool geometry on mechanical and microstructural properties of friction-stir-welded 1050-H24, 6061-T6, and 5083-O aluminum plates. Recently, the present authors [18] showed that a stepped conical threaded pin gives more homogeneous and defect-free joints. Therefore, the geometrical characteristics of the tool including shoulder and pin diameter, the transition zone between the shoulder and the pin, diameter and profile of the pin, and thread size and height influence the quality of the weld joint and particularly the elimination of the kissing bond defect.

Among all aluminum alloy series, the non-heat-treatable Al–Mg alloys (5xxx series) are the most suitable material for marine applications because of their combined high strength and excellent corrosion resistance [5, 19]. For example, AA5456 is being used for deck floor and wall structures by the US coast guard for its rescue boats which often work under very severe conditions [19]. While relatively extensive data exist on FSW of 2xxx, 7xxx, and 6xxx series aluminum alloys probably because of the historical application of FSW

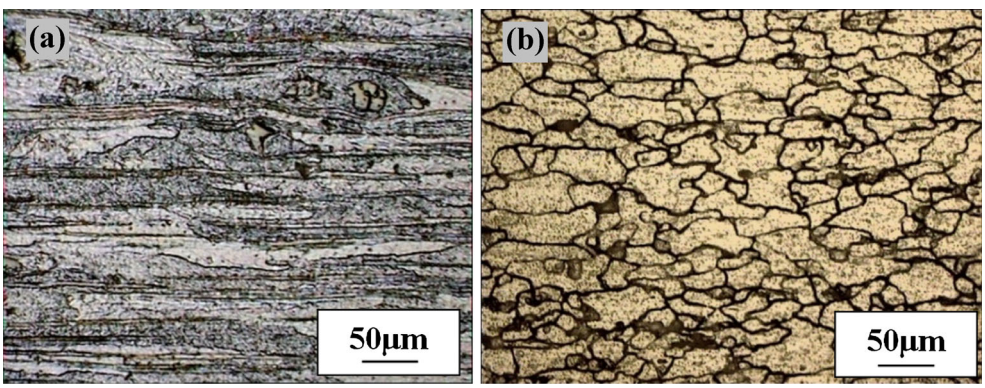

Fig. 1 Microstructure of base metal **a** cold worked plate and **b** annealed plate

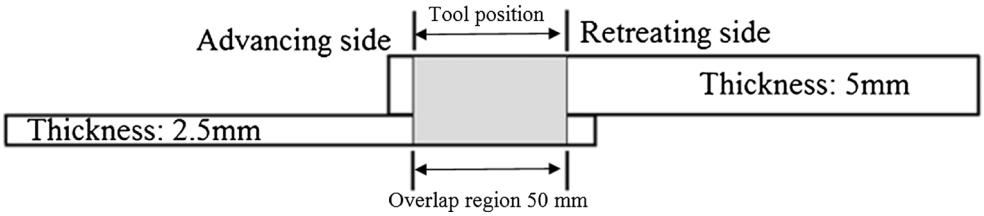

Fig. 2 Schematic of the lap mode set up for FSW experiments

technology to aerospace-grade alloys, little information is available on FSW of 5xxx series alloys.

Microstructure, mechanical properties, and corrosion behavior of FSW butt joints of Al 5456 have been investigated [7, 8]. Especially, the influence of weld process parameters on grain growth and precipitate evolution was discussed [7, 8]. Also, the effect of environmental conditions (such as laboratory air, water vapor, and oxygen) on fatigue crack growth of FSWed 5456–H116 alloy has been investigated [7]. However, very little has been reported on FSW lap joint configuration of this alloy. These types of joints are commonly used for assembling different structural components in the transportation industry such as ship decks, walls, railway tankers, and wagons [3, 4, 18, 20]. The data become even less available when dissimilar welding conditions (material thickness or conditions) are considered [18].

The present paper aims to study the characteristics of microstructure, related defects, and mechanical properties (microhardness) of FSW lap joints with different material thickness and temper conditions. Also, four different tool geometry types and two rotational speeds are used to better quantify the impact of tool geometry and simulate near to industrial conditions by using different rotational speeds. From an industrial application perspective, the main objective of the project was to determine the optimum processing conditions to achieve defect-free welds with the highest mechanical properties.

From a fundamental point of view, the present results will also contribute to a better understanding of microstructure evolution of this alloy under high strain and strain rate conditions which are not presentably available in the literature. Finally, the results of this investigation could be used as a basis for other researchers working on numerical simulation of the FSW process, as quantifying the influence of tool geometry on mechanical properties and defect characteristics will help to better model material flow in the nugget zone of the weld joint.

2 Material and experimental procedure

Two AA 5456 aluminum alloy plates with different thicknesses were friction-stir-welded in lap configuration. The upper plate was 5-mm-thick cold worked AA5456-T321 alloy and the lower plate was made of 2.5-mm-thick annealed sheets of AA5456. The chemical compositions of the

Fig. 3 Technical details of the utilized tools

Tools	Description of the pin	Big diameter of the pin (mm)	Small diameter of the pin(mm)	Pitch of the pin(mm)
T1	Conical screw thread pin	7	5	0.8
T2	Cylindrical–conical thread pin	7	5	0.8
T3	Stepped conical thread pin	7.5	4	0.8
T4	Neutral Flared-Triflute pin	7	5	0.8

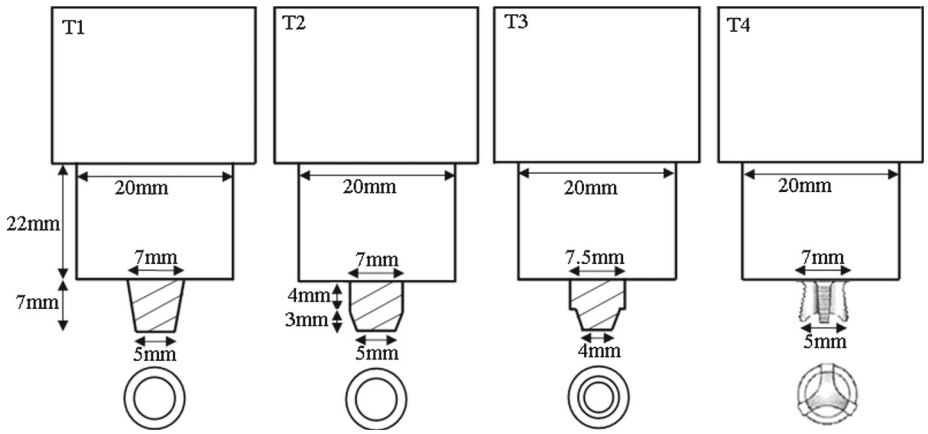

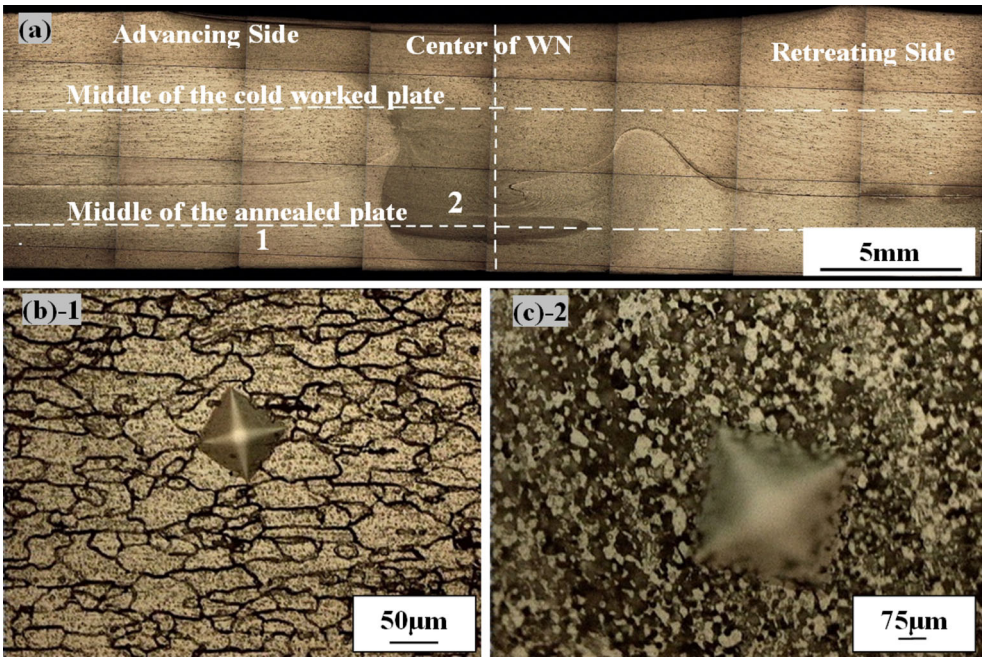

Fig. 4 **a** Schematic of the microhardness position, **b** microhardness spot on the lower base plate, and **c** microhardness spot on lower WN

investigated materials are shown in Table 1, and the microstructures of the as-received materials are presented in Fig. 1.

Test coupons with dimension of 250×250 mm^2 were cut out in the rolling direction from the as-received materials. The test pieces were first ground using a steel brush and sandpaper to remove the oxide film and then cleaned with acetone to remove any organic residues before friction stir welding. The specimens were arranged in a lap mode with 50-mm overlap relative to the welding and tool rotation directions with the advancing side of the pin near the edge of the upper workpiece (ANE). Figure 2 shows schematically the welding assembly.

The geometrical details of the four tools used in the investigations are shown in Fig. 3. A conical screw thread pin (T1), a cylindrical–conical thread pin (T2), a stepped conical thread pin (T3), and neutral flared-triflute (T4) pin tool were used. The pin length was 7 mm and the shoulder diameter was 20 mm. The shoulder underside surface was flatted and the tilting angle of the probe tool was 3° for all the experiments. Both the shoulder and probe were made of H13 steel. The welding direction was perpendicular to the rolling direction of the workpieces, and all the lap joints were produced at a travel speed of 30 mm/min. Two tool rotational speeds, 600 and 800 rpm, were used in the

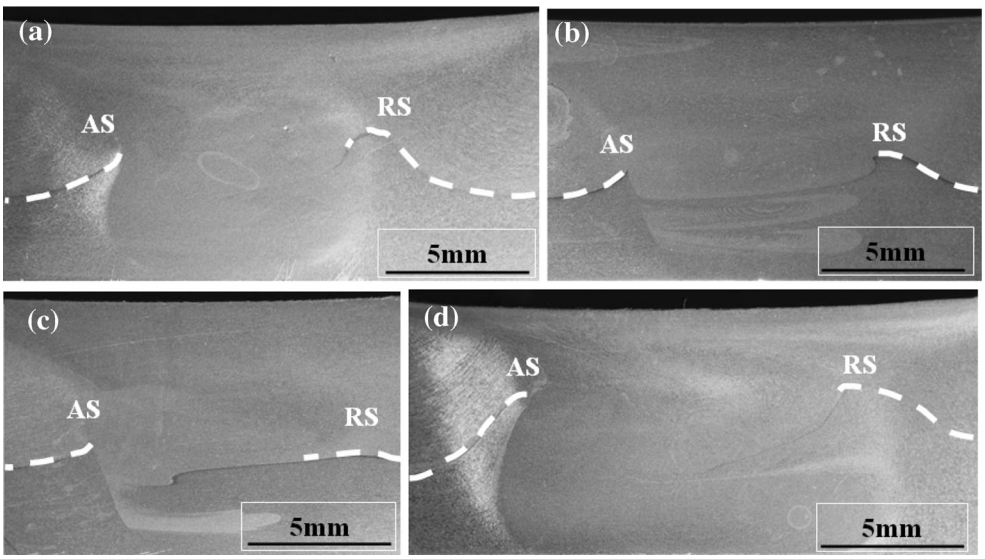

Fig. 5 Macro cross sections of the WN for rotational speed of 600 rpm, welded by **a** T1, **b** T2, **c** T3, and **d** T4 tools (*AS* advancing side, *RS* retreating side)

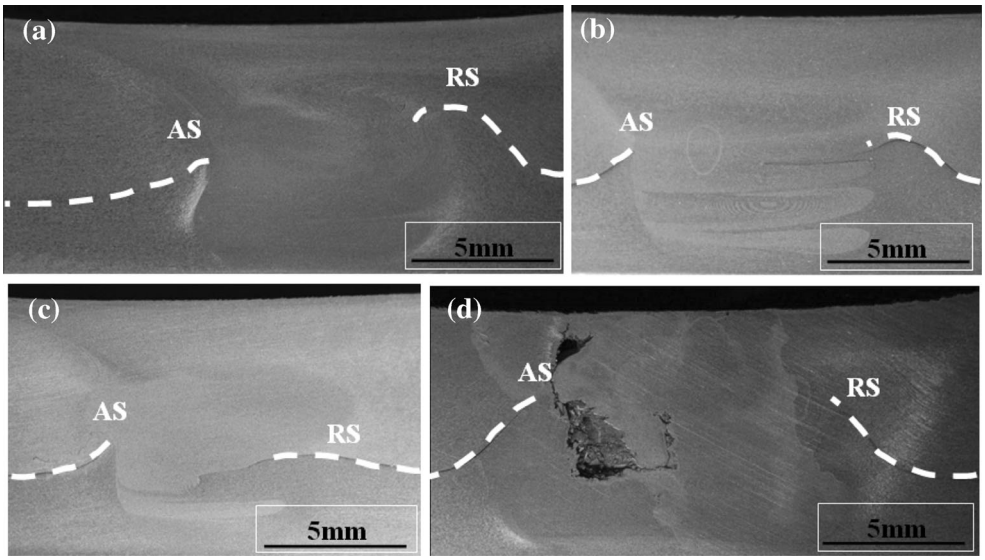

Fig. 6 Macro cross sections of the WN for rotational speed of 800 rpm, welded by **a** T1, **b** T2, **c** T3, and **d** T4 tools (*AS* advancing side, *RS* retreating side)

study. It must be noted that other authors have used similar geometry types to that of the T1 (conical screw thread pin), T2 (cylindrical–conical thread pin), and T4 (neutral flared triflute) [4, 5, 8] for butt or lap joints; however, the geometry of the T3 (stepped conical thread pin) tool is a new design that is used for the first time by the present authors.

Following FSW, test specimens were machined out according to the AWS D17.3M:200X standard. Transverse sections were polished using standard metallographic procedures and etched using a solution composed of 35 ml HNO_3 and 65 ml H_2O under at 80 °C. Microhardness measurements were performed using an Olympus automated microindentation hardness testing system at the center of the upper and lower plates and through the thickness in the WN along the dotted line shown in Fig. 4. A load of 200 g and a dwell time of 15 s were used for microhardness measurements (Fig. 4b, c). For grain size measurements, manual one-phase intercept method was used.

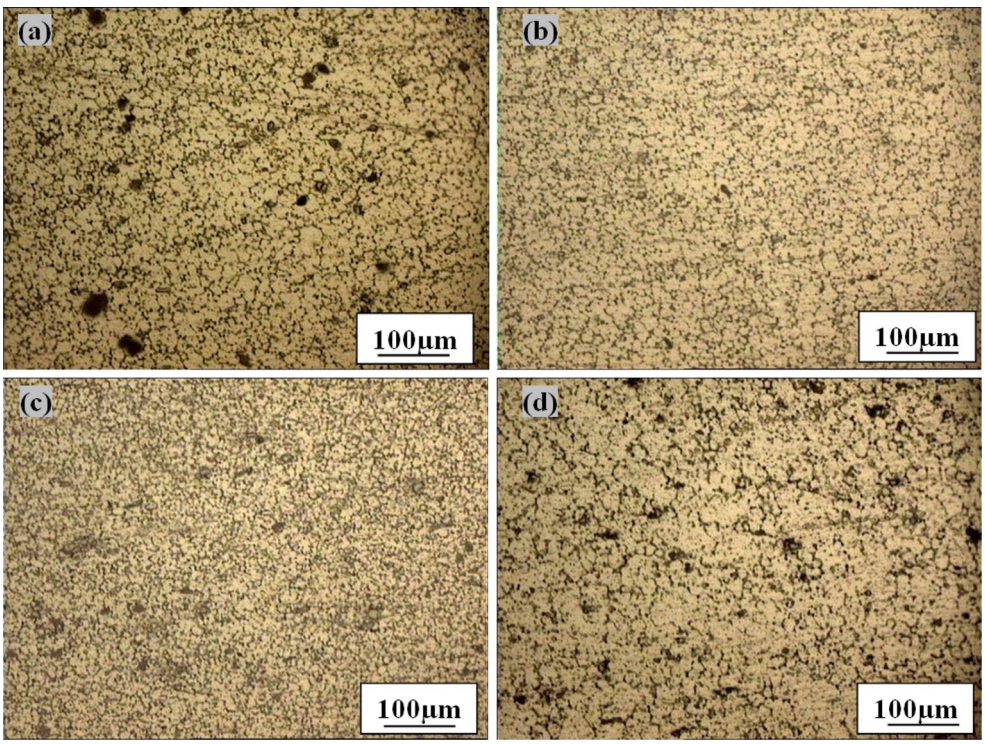

Fig. 7 Microstructures in the center of the WN zone for rotational speed of 600 rpm welded by **a** T1, **b** T2, **c** T3, and **d** T4 tools

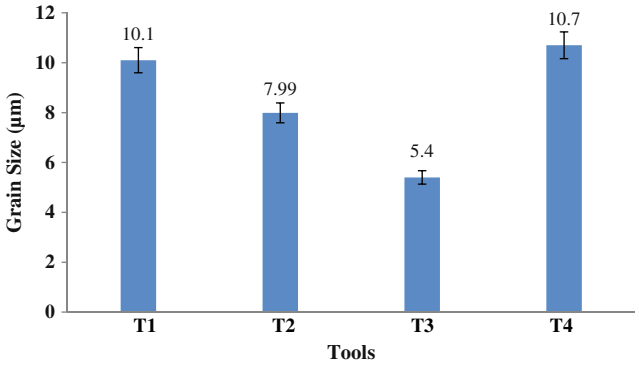

Fig. 8 Grain size variation versus tool geometry indicating that the stepped conical thread pin has the largest grain refinement effect

3 Results and discussion

3.1 Microstructure evolution with pin geometry

Macrographs of weld joint cross sections obtained with the four investigated tools and under rotational speeds of 600 and 800 rpm are shown in Figs. 5 and 6, respectively. The specimens were selected from the weld regions without apparent defects at their surface. The presence of the hooking defect with different height and intensities can be observed in these joints. For tool T4 and 800 rpm, a void defect is also observed just below the surface. These observations could be analyzed in terms of the influence of tool geometry on material plastic flow. Indeed, under similar welding conditions, the heat input and material flow under the shoulder depend on pin profile. Higher heat input will improve plasticity and higher forge force will be more effective in transferring the material from the advancing side to the retreating side of the joint. As illustrated in Fig. 6d, such conditions are not satisfied for welding conditions with the T4 tool at 800 rpm. It can be seen that insufficient material flow from the retreating side to the advancing side resulted in the formation of void defect.

Figure 7 shows the corresponding microstructures in the WN zone in the upper plate for the four tools and for rotational speed of 600 rpm. A comparison of the obtained microstructures indicates that for all four conditions, the nugget region has experienced high temperatures and extensive plastic deformation. The average grain size in the WN produced by T1, T2, T3, and T4 was measured and is 10.1, 7.9, 5.4, and 10.7 µm, respectively (Fig. 8). The results clearly illustrate the influence of pin geometry on microstructure evolution, and it appears that the T3 tool has the largest grain-refining effect.

Microstructural changes in the transition from the WN to the TMAZ on the advancing side are shown in Fig. 9. As it can be seen, for all experimental conditions, the grain size in the WN is much finer than that in the TMAZ and with an abrupt change from one zone to another for tools 1 and 2, while the transition is more gradual in the case of tool T3 (Fig. 9c) and tool 4 (Fig. 9d). Specifically, in Fig. 9c, near the nugget zone, the microstructure of the advancing side consists of small, relatively equiaxed grains with grain sizes ranging from 4.4 to 7.7 µm. By contrast, in the TMAZ, close to the weld

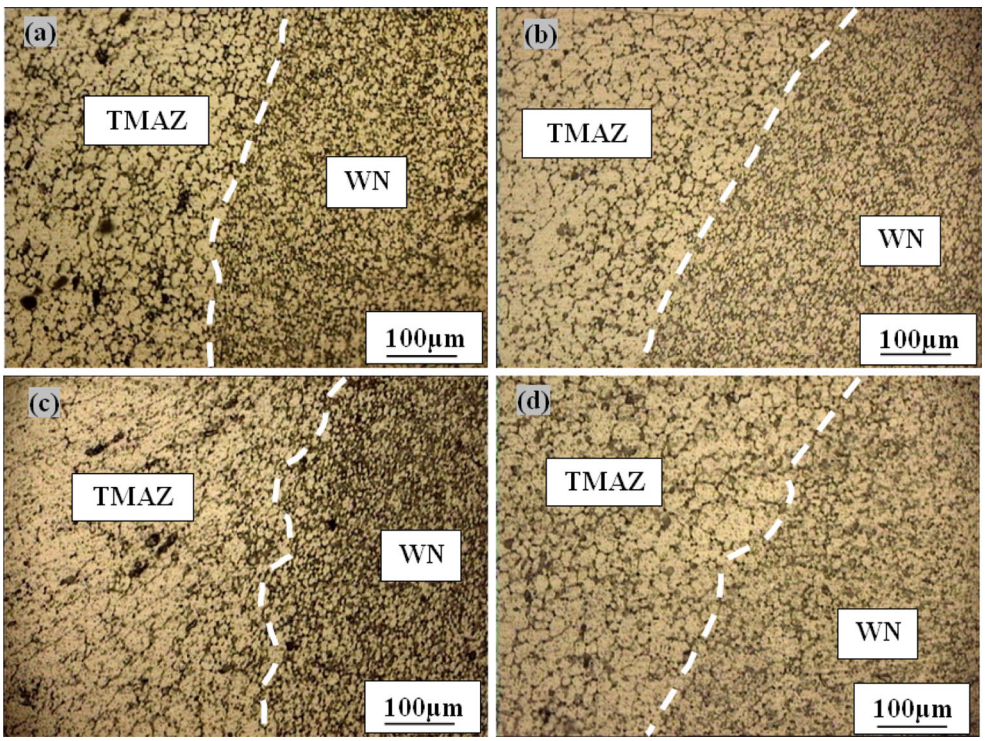

Fig. 9 Microstructures in WN–TMAZ under rotational speed of 600 rpm on the advancing side, welded by **a** T1, **b** T2, **c** T3, and **d** T4

nugget, elongated grains with average grain sizes in the range 9.4 to 14.5 μm were observed. The TMAZ zone is a specific characteristic of friction-stir-welded joints. This region is located at the frontier of the weld nugget and therefore is submitted to a certain amount of deformation; however, it is widely accepted that the amount of deformation is not enough to induce any microstructural changes such as recrystallization [21–23]. Therefore, it can be reasonably assumed that in the present investigation, the TMAZ has also experienced significantly lower deformation and has not gone through recrystallization.

Microstructure evolution in the retreating side (as shown in Fig. 10) is more complicated due to the complex flow of the extruded metal, and as a result, no obvious and apparent boundary between the WN and TMAZ could be clearly distinguished.

3.2 Microhardness evolution

Hardness evolution as a function of position in the joint and as well as tool geometry was investigated. An illustrative example is shown in Fig. 11 where hardness changes measured along the weld center line are presented. It can be seen that although the starting hardness level of the two alloys is significantly different (highly cold worked, high hardness for the upper plate versus annealed and softer for the lower plate), the two materials have the same levels of hardness in the WN. Specifically, the upper base metal has hardness of about 140 HV which is very high for an alloy of this type compared to 85 HV for the lower plate. By contrast, inside the weld nugget zone, the hardness value drops to about 93 HV despite the much fine grain structure when compared to the base metal (Figs. 1 and 7). The finer grains sizes in the nugget zone can be attributed to the occurrence of dynamic recrystallization during material mixing. Lower hardness in WN can be attributed

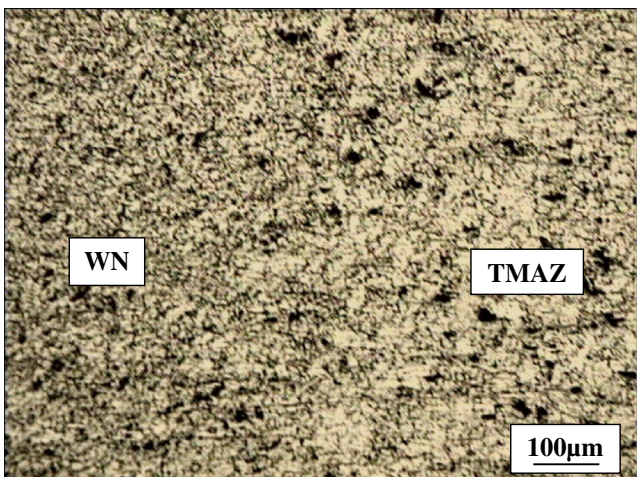

Fig. 10 Microstructure in the transition region of WN–TMAZ, T3 tool rotational speed of 600 rpm, and retreating side of the weld

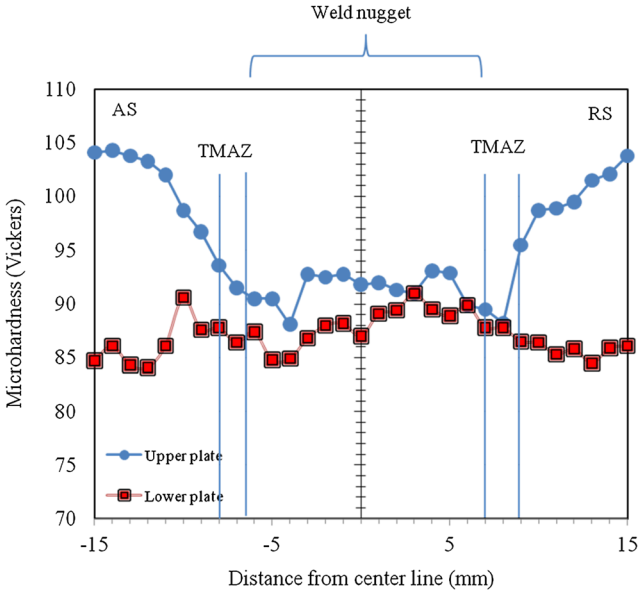

Fig. 11 Microhardness profile across the center line of the weld upper and lower plates for the T2 tool, 600 rpm, and 30 mm/min welding speed

to the precipitate dissolution [24] or dislocation annihilation [25].

Outside the weld nugget area and inside the TMAZ, the microhardness values increase gradually but with small fluctuations. The observed fluctuations are probably due to heterogeneous deformation, characteristic of TMAZ, which results in non-uniform grain size and uneven microhardness. Also, some abrupt drops are locally observed, which are probably due to the partial mixing of the softer lower plate material with the harder upper plate. Indeed, during FSW lap welding, the material of the lower plate is pushed up toward the upper one [19]. While temperature and deformation in the WN are high enough for complete mixing of the two materials, in the TMAZ, such

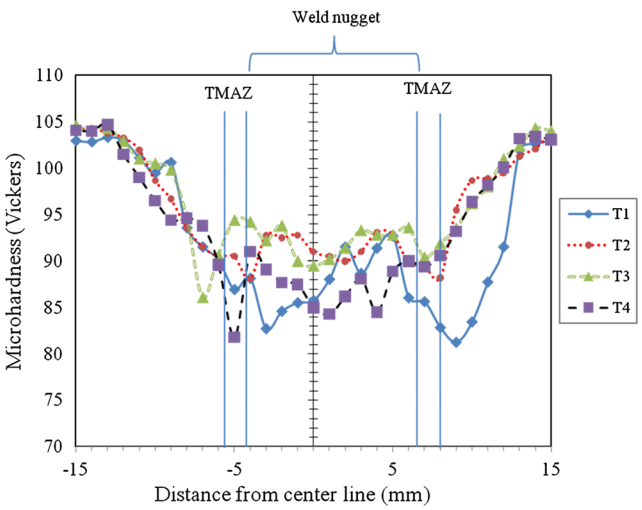

Fig. 12 Microhardness across the WNZ in cold worked plate by using four different pin geometry types, under 600 rpm of rotational speed and 30 mm/min welding speed

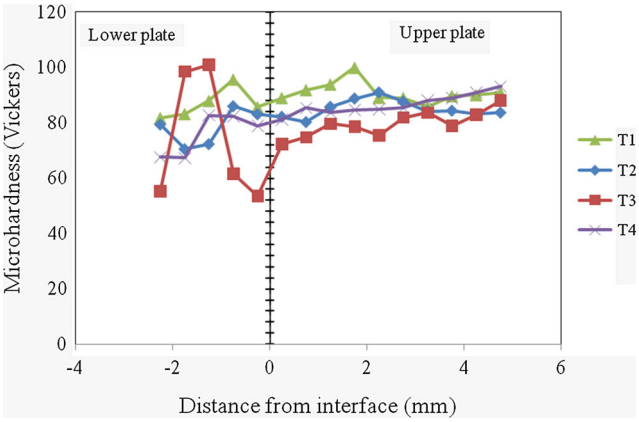

Fig. 13 Microhardness through the thickness in the WN using four different pin geometry types, 600 rpm, and 30 mm/min of welding speed

conditions are not often produced and stray of lower plate material exists unmixed within the upper plate material resulting in heterogeneous behavior in mechanical properties. Finally, hardness values gradually increase from TMAZ to HAZ and then reach their maximum value in the base metal.

Microhardness profiles along the center line of the weld joints made by the four tools and 600-rpm rotational speed are shown in Fig. 12. As observed, maximum hardness values in the nugget zone are obtained in the joints produced using T3. This is probably related to improved deformation conditions obtained with the T3 tool which resulted in finer grain sizes (5.2 μm) as previously illustrated in Figs. 7c and 8.

Figure 13 shows the microhardness values and Fig. 14 displays the microstructure of the FSW region of all lap-welded joints fabricated using the four tools, each with specific pin profile, for comparison purposes. Microhardness profiles were investigated through the thickness of the weld in the weld nugget regions. The results indicate that the region of the weld nugget located in the upper plate suffers bigger amount of plastic deformation and centrifugal forces than the one in the lower plate [18]. As a result, the stir zone in the upper plate has a more uniform structure and consequently similar hardness. As depicted in Fig. 13, the microhardness profile in the cold worked plate is almost uniform and very close together for the four investigated tool geometry types. By contrast, more important variations are observed in the microhardness profiles

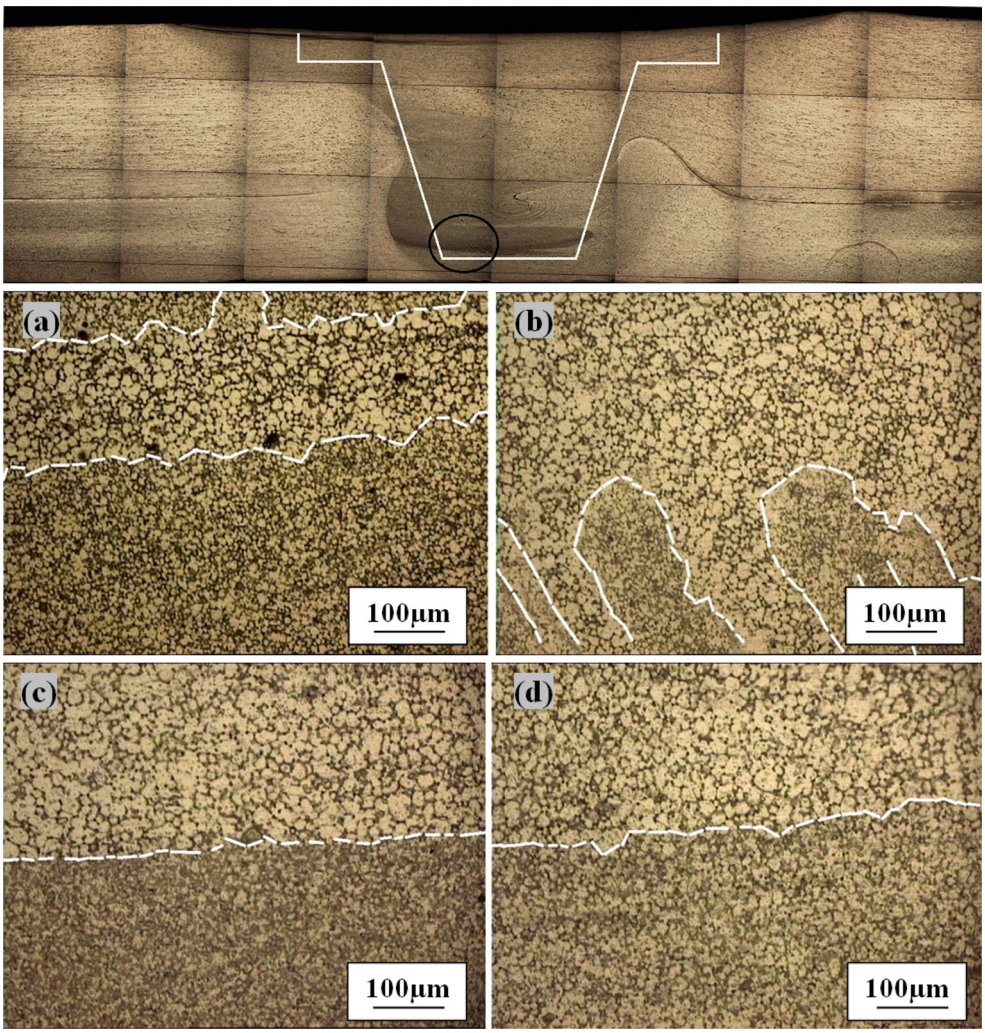

Fig. 14 Optical micrographs showing the microstructures in the lower regions (*bottom*) of the nugget zone, welded by **a** T1, **b** T2, **c** T3, and **d** T4 tools, rotational speed 600 rpm and travel speed 30 mm/min (images have been taken from the *black circled area* of the nugget zone)

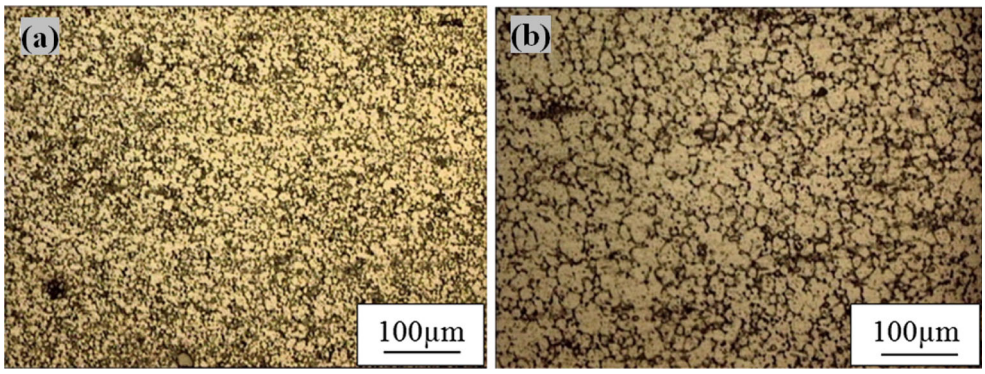

Fig. 15 Optical micrographs of the central regions of WN on cross sections perpendicular to the welding direction for rotation speeds of **a** 600 and **b** 800 rpm, using the T3 tool

in the lower plate. These variations are probably related to different material flow patterns induced by geometrical features of each tool. Also, hardness evolution in the annealed plate (lower plate) for the joints produced using T1, T2, and T4 tools is more uniform and approximately similar, whereas the weld joint produced using the T3 tool displays the largest variation of microhardness.

The influence of precipitate distribution on microhardness profile has been reported by several authors in recent years [11, 14, 15]. The influence has been related to the amount of heat introduced locally in the WN during FSW. The severity of this heat input has been mainly related to the contact surface between the tool and the material [11, 26]. The generated heat combined with the severe deformation affects the kinetics of recrystallization, grain and precipitates' size evolution, and therefore hardness profile. Finally, it must be mentioned that the highest levels of microhardness were obtained in the WN of joints produced using the T3 tool in the annealed plate (lower plate). The obtained values for microhardness in the WN zone are coherent with other microstructural parameters such as finer grain size.

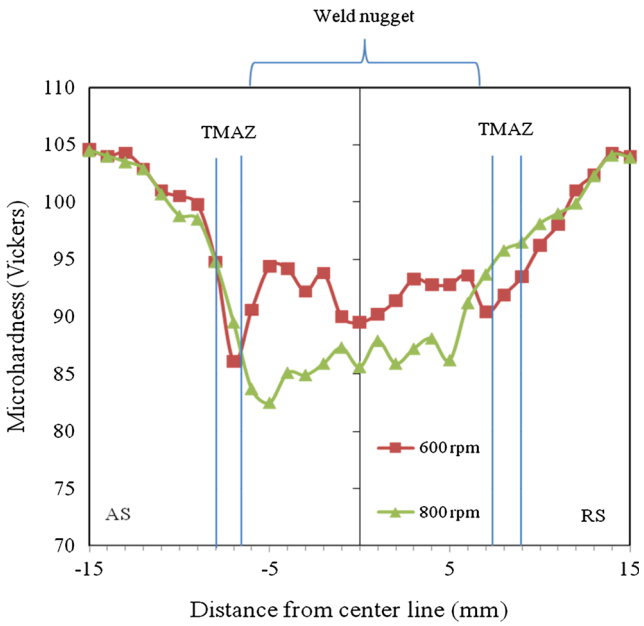

Fig. 16 Microhardness at mid-thickness in the WN on cold worked plate at different rotation speeds welded by the T3 tool and at 30 mm/min welding speed

Figure 14 shows the microstructure of the stir zone at the bottom of the weld nugget in the lower plate for the four investigated tools. As depicted, uneven and banded microstructures are obtained. The different grain sizes and variable microstructures are mainly due to different material mixing at the bottom of the tool originating from the specific geometry of each tool. The obtained results clearly reveal that material extrusion at the bottom of the weld and hence its characteristics (microstructure. hardness, defect generation) are strongly dependent on tool geometry.

3.3 Effect of tool rotational speed

Rotational speed is one of the most important process variables in FSW influencing the deformation rate and the total strain imposed on the material for a given weld speed. Specifically, rotational speed influences the recrystallization process and grain growth. The higher the rotational speed is, the higher the extent of recrystallization would be (i.e., higher heat input). By contrast, lower heat input conditions due to lower rotational speed result in lack of stirring, decrease the size of the weld nugget, and finally affect the mechanical properties of the weld joint.

Figure 15 shows the microstructures of the WN on cross sections perpendicular to the welding direction for the two rotation speeds of 600 and 800 rpm using the T3 tool. The stir zone is comprised of small and equiaxed grains as a result of severe plastic deformation and grain refinement due to dynamic recrystallization. The results indicate that the average grain size increases from 6.8 to 12.1 μm with increasing tool rotation speed demonstrating the occurrence of grain growth due to more heat input introduced at the higher rotational speed. The impact of employing higher rotational speed on mechanical properties is illustrated in Fig. 16 where it can be seen that the central region of the nugget zone has significantly lower microhardness levels when the higher rotational speed is used.

4 Conclusions

Friction stir welding of 5456 Al alloys in lap configuration, two different thicknesses, and different microstructures (temper conditions) was investigated. Four different friction stir pins were designed to study the influence of the pin geometry on the weld shape and structural and mechanical properties. The following conclusion can be drawn from the present study:

1. The geometry of the pin has a significant influence on the joint microstructure and its mechanical properties. Pin geometry strongly affects the plastic flow of the material resulting in different material extrusion paths. The optimum results were obtained using the stepped conical thread pin tool (T3 tool). The weld joints were characterized by smooth surface quality, no obvious defects, uniform microstructure, and fine grain size in the weld nugget.
2. Of the two tool rotational speeds used in this investigation, the ones fabricated at rotational speed of 600 rpm showed better mechanical properties, irrespective of tool pin profiles.
3. For the four investigated tool geometry types, higher rotational speeds result in grain growth and a drop in mechanical properties.

References

1. Buffa G, Campanile G, Fratini L, Prisco A (2009) Friction stir welding of lap joints: influence of process parameters on the metallurgical and mechanical properties. Mater Sci Eng A 519:19–26
2. Zhao YH, Lin SB, Wu L, Qu FX (2005) The influence of pin geometry on bonding and mechanical properties in friction stir weld 2014 Al alloy. Mater Lett 59:2948–2952
3. Cederqvist L, Reynolds AP (2001) Factors affecting the properties of friction stir welded aluminum lap joints. Weld J Res Suppl 80–12:281–287
4. Fleming PA, Hendricks CE, Cook GE, Wilkes DM, Strauss AM, Lammlein DH (2010) Seam-tracking for friction stir welded lap joints. ASM Int JMEPEG 19:1128–1132
5. Chionopoulos SK, Sarafoglou CI, Pantelis DI, Papazoglou VJ (2008) Effect of tool pin and welding parameters on friction stir welded (FSW) marine aluminum alloys. Proceedings of 3rd ICME N, Chalkidiki :307–316
6. Chen HB, Yan K, Lin T, Chen SB, Jiang CY, Zhao Y (2006) The investigation of typical welding defects for 5456 aluminum alloy friction stir welds. Mater Sci Eng A 433:64–69
7. Menzemer C, Srivatsan TS (1999) The effect of environment on fatigue crack growth behavior of aluminum alloy 5456. Mater Sci Eng A 271:188–195
8. Fonda RW, Pao PS, Jones HN, Feng CR, Connolly BJ, Davenport AJ (2009) Microstructure, mechanical properties, and corrosion of friction stir welded Al 5456. Mater Sci Eng A 519:1–8
9. Bahemmat P, Rahbari A, Haghpanahi M, Besharati MK (2008) Experimental study on the effect of rotational speed and tool pin profile on AA2024 aluminum friction stir welded but joints. Proceedings of ECTC, ASME technical conference, Miami, Florida, USA: 1.1–1.7
10. Leal RM, Loureiro A (2008) Effect of overlapping friction stir welding passes in the quality of welds of aluminum alloys. Mater Design 29:982–991
11. Scialpi A, De Filippis LAC, Cavaliere P (2007) Influence of shoulder geometry on microstructure and mechanical properties of friction stir welded 6082 aluminum alloy. Mater Design 28:1124–1129
12. Fujii H, Cui L, Maeda M, Nogi K (2006) Effect of tool shape on mechanical properties and microstructure of friction stir welded aluminum alloys. Mater Sci Eng A 419:25–31
13. Elangovan K, Balasubramanian V (2007) Influences of pin profile and rotational speed of the tool on the formation of friction stir processing zone in AA2219 aluminum alloy. Mater Sci Eng A 459:7–18
14. Boz M, Kurt A (2004) The influence of stirrer geometry on bonding and mechanical properties in friction stirs welding process. Mater Design 25:343–347
15. Elangovan K, Balasubramanian V (2008) Influences of tool pin profile and tool shoulder diameter on the formation of friction stir processing zone in AA6061 aluminium alloy. Mater Design 29: 362–373
16. Oosterkamp A, Oosterkamp LD, Nordeide A (2004) 'Kissing bond' phenomena in solid-state welds of aluminum alloys. Weld J 83: 225S–231S
17. Zhou C, Yang X, Luan G (2006) Effect of kissing bond on fatigue behavior of friction stir welds on Al 5083 alloy. J Mater Sci 41: 2771–2777
18. Salari E, Jahazi M, Khodabandeh A, Ghasemi-Nanesa H (2014) Influence of tool geometry and rotational speed on mechanical properties and defect formation in friction stir lap welded 5456 aluminum alloy sheets. Mater Design 58:381–389
19. Kallee S (2000) Application of friction stir welding in the shipbuilding industry. Paper presented at the Lightweight construction. The Royal Institution of Naval Architects, TWI, Cambridge, UK, 25–25 February 2000
20. Dubourg L, Merati A, Jahazi M (2010) Process optimization and mechanical properties of friction stir lap welds of 7075-T6 stringers on 2024-T3 skin. Mater Design 31–7:3324–3330
21. Afrin N, Chen DL, Cao X, Jahazi M (2008) Microstructure and tensile properties of friction stir welded AZ31B magnesium alloy. Mater Sci Eng A 472(1–2):179–186
22. Cavaliere P, De Santis A, Panella F, Squillace A (2009) Effect of welding parameters on mechanical and microstructural properties of dissimilar AA6082–AA2024 joints produced by friction stir welding. Mater Design 30(3):609–616
23. Liu HJ, Fujii H, Nogi K (2004) Microstructure and mechanical properties of friction stir welded joints of AC4A cast aluminium alloy. Mater Sci Tech 20(3):399–402
24. Chen YC, Feng JC, Liu HJ (2009) Precipitate evolution in friction stir welding of 2219-T6 aluminum alloys. Mater Charact 60:476–481
25. Sukedai E, Yokoyama T, Song M (2014) Microstructure and tensile properties of a friction stir welded Al–Mg–Si alloy. Int J Mater Res 105(9):883–893
26. Gemme F, Verreman Y, Dubourg L, Jahazi M (2010) Numerical analysis of the dwell phase in friction stir welding and comparison with experimental data. Mater Sci Eng A 527(16–17):4152–4160